frontiers | Frontiers in Biomaterials Science

TYPE Original Research
PUBLISHED 20 June 2025
DOI 10.3389/fbiom.2025.1394166

OPEN ACCESS

EDITED BY
Hua Wang,
Shandong University, China

REVIEWED BY
Valeriya Kudryavtseva,
Queen Mary University of London, United Kingdom
Chun Wang,
University of Minnesota, United States

*CORRESPONDENCE
Ken Gall,
kag70@duke.edu

RECEIVED 01 March 2024
ACCEPTED 26 May 2025
PUBLISHED 20 June 2025

CITATION
Abar B, Goonewardene H, Sheng R, Negus MH, Allen NB, Kelly CN, Stinson NC, Becker ML, Thaden JT, Adams SB and Gall K (2025) A 3D-printed, high-strength, and drug-eluting composite for the treatment of periprosthetic joint infections.
Front. Biomater. Sci. 4:1394166.
doi: 10.3389/fbiom.2025.1394166

A 3D-printed, high-strength, and drug-eluting composite for the treatment of periprosthetic joint infections

Bijan Abar[1,2], Harrison Goonewardene[1], Richard Sheng[1], Mitchell H. Negus[1], Nicholas B. Allen[2], Cambre N. Kelly[1], Natasha C. Stinson[1], Matthew L. Becker[1], Joshua T. Thaden[3], Samuel B. Adams[2] and Ken Gall[1]*

[1]Department of Mechanical Engineering and Material Sciences, Duke University, Durham, NC, United States, [2]Department of Orthopaedic Surgery, Duke University, Durham, NC, United States, [3]Duke University, Division of Infectious Diseases, Duke University, Durham, NC, United States

Introduction: Periprosthetic joint infections are relatively rare complications of total joint replacements. The standard of care for these infections involves the placement of a temporary spacer made of poly (methyl methacrylate) (PMMA) bone cement combined with antibiotics. The rate of major complication can be as high as 12% for PMMA spacers. Therefore, this study was designed to identify an alternative resin material that could be 3D printed, provide mechanical support necessary for ambulation, and deliver a therapeutic dose of antibiotics over an extended period.

Methods: Test substrates were photochemically printed out of Biomed Clear (BMC) loaded with up to 16% gentamicin or 10% vancomycin (wt%). PMMA and BMC composites were characterized using differential scanning calorimetry, dynamic mechanical analysis, compression testing, and a 30-day antibiotic elution study.

Results: The thermoset properties of the BMC allowed for the compressive properties to remain unchanged (post-elution = compressive strength 84–94 MPa) as antibiotics were added to the resin (0–16 wt%). However, antibiotic elution was influenced by the type and concentration of the antibiotic in the composite. In contrast, the thermoplastic properties of PMMA led to a decrease in compressive properties with the addition of antibiotics, but PMMA was able to elute relatively more antibiotics.

Discussion: This study described a novel method to 3D print load bearing materials that can release antibiotics over 30 days. BMC composites have some advantages and disadvantages compared to PMMA that need to be considered when developing new treatments for orthopaedic infections.

KEYWORDS

PMMA, 3D printing, patient-specific implants, drug elution, mechanical testing, periprosthetic joint infections, antibiotics, orthopaedic

1 Introduction

As of 2010, 2.5 million Americans have received total hip replacements (THR) and 4.7 million Americans have received total knee replacements (TKR) (Kremers et al., 2015). When an infection develops on the metal implant surface, bacteria can form a treatment resistant biofilm known as a periprosthetic joint infection (PJI) (McConoughey et al., 2014). For total hip and knee replacements, the 1-year incidence rate of PJI is 0.25%–2% in primary surgeries and 3.2%–5.6% in revisions (Gbejuade et al., 2015). If left untreated, PJIs may spread throughout the body, leaving the limb unsalvageable and requiring amputation (Eckers et al., 2021).

An integral component to PJI treatment is the delivery of antibiotics. After removal of the infected hardware and surgical debridement of the surrounding infected tissue, the residual infection needs to be cleared to prevent risk for repeat PJI in the replacement metal implant (Li et al., 2018). The current standard of care in PJI for antibiotic delivery is a temporary cement spacer loaded with antibiotic. The spacer is made out of poly (methyl methacrylate) (PMMA), and gentamicin, a broad-spectrum antibiotic (von Hertzberg-Boelch et al., 2022). As part of a two-stage exchange arthroplasty, the spacers are molded into the shape of the removed implant and placed during the initial debridement procedure (Li et al., 2023). The spacers release antibiotics to kill the remaining bacteria locally with at least 6 weeks of systemic antibiotics, while providing mechanical support that increases patient mobility until a definitive replacement implant can be placed (Charette and Melnic, 2018).

Complications include spacer dislocation/fracture, periprosthetic fracture, and persistent infection (Li et al., 2021). As spacers are pre-made with varying generic sizes, trial spacers are required to test optimal fit intraoperatively. The sub-optimal anatomic fit can result in spacer dislocation and subsequent implant fracture from new stress concentrations. A study examining 155 articulating knee spacers found that 24% were tilted, 21% had medio-lateral translation, and 12% had major complications like fracture, spacer dislocation, or knee subluxation (Struelens et al., 2013). To solve this problem, some surgeons use CT-scan based 3D-printed molds. However, this process can be difficult as these molds have to be filled in the operating room in sterile conditions. Within minutes after mixing the PMMA components, the surgeon must mold the PMMA and wait for it to set, thus adding additional back table time and subjecting the patient to additional anesthesia. The only FDA cleared spacers use gentamicin. However, gentamicin is relatively ineffective against Gram-positive bacteria commonly seen in PJI such as *Staphylococcus epidermidis* (SA) *or Methicillin-resistant Staphylococcus aureus* (MRSA). 41% of staphylococci isolated from PJI patients were resistant to gentamicin (Anguita-Alonso et al., 2005). Therefore, there is an unmet need to create a biocompatible and patient-specific spacer that provides the mechanical support needed for ambulation and delivers a therapeutic dose of the specific antibiotic that is most effective in treating the infection.

2 Materials and methods

2.1 Fabrication of samples

Cylinders that had a diameter of 6 mm and a height of 12 mm were either 3D-printed with a photoresin or molded out of PMMA-based bone cement (PALACOS® R), as shown in Figure 1. The 3D-printed samples were created via stereolithography (SLA), which allowed for antibiotics to be incorporated into photoresin. A computer-aided design (CAD) model of the cylinder was sliced into thin 100 μm 2D layers and uploaded into the Form 2 3D printer (Formlabs). Biomed clear (BMC), a biocompatible liquid photoresin from Formlabs was used as the printing material. The commercially available resin that has been evaluated in accordance with ISO 10993–1:2018, ISO 7405:2018, ISO 18562–1:2017 and have passed the requirements associated with being not cytotoxic, not an irritant, not a sensitizer, not toxic (subacute/subchronic), not mutagenic, non-pyrogenic, and not systemically toxic (BioMed Clear Resin, 2024). The BMC was then doped with varying amounts of gentamicin sulfate (VWR) or vancomycin hydrochloride (VWR). The measured amount of antibiotic powder was added to a beaker filled with the printing resin. An immersion blender was used to create a homogeneous mixture, which was then poured into the printing vat. The printing process began shortly afterward to ensure the antibiotic powder remained evenly suspended in the solution. The concentration of gentamicin ranged from 0%–16% (W/W) and the concentration of vancomycin ranged from 0%–10% (W/W). A build plate was lowered into the vat where a laser selectively polymerizes the liquid resin into a solid. The build plate was lifted, and the process was repeated in a layer-wise fashion until the print was complete (Pagac et al., 2021). After the samples were printed, they were washed in fresh Isopropyl Alcohol (VWR) for 20 min, and cured at 60°C for 60 min. Both gentamicin and vancomycin were chosen because they have been clinically used in antibiotic PMMA spacers where they have been found to be heat stable in the exothermic curing process that can reach 115°C (Carli et al., 2018; Chen et al., 2019). Additionally, preliminary studies showed that the eluted gentamicin and vancomycin were still functional enough to kill bacteria plated on a Petri dish following the extensive processing required to make a 3D print.

PMMA samples were made with commercial bone cement containing PMMA copolymer (84%), zirconium dioxide (15%) and benzoyl peroxide (1%) in the powder component, and methyl methacrylate (98%) and N, N-dimethyl-p-toluidine (2%) in the liquid component. Either gentamicin or vancomycin were thoroughly mixed by hand into 2000 mg of the dry powder so the W/W percentage of antibiotics and PMMA bone cement (dry + liquid mass) was equivalent to BMC samples when 1 mL of liquid monomer was added. The samples were mixed until uniform and was transferred to a 3 mm slip tip syringe. The bone cement was then injected into cylindrical molds that were machined out of Delrin blocks (Mcmaster Carr). After 20 min, the cylindrical samples were tapped out of the molds using a brass punch. The flat face of the BMC and PMMA cylinders were polished with sandpaper to a final height of 12 mm.

The composites were referred to by their base material and the weight percentage of antibiotic. For example, BMC 2G represents a BMC composite doped with 2% gentamicin, and PMMA 10V represents a PMMA composite doped with 10% vancomycin.

2.2 Differential scanning calorimetry

The thermodynamic properties of BMC-G and PMMA composite were assessed using Differential Scanning Calorimetry (DSC) (Gill et al., 2010). 4 pieces of each sample (5–10 mg) were cut from a rectangular bar of printed BMC or molded PMMA. The samples were sealed in an aluminum hermetic pan and placed in a TA Discovery 2500 DSC machine. The samples were cycled twice between −60°C and +150° at a rate of 10°C/min. The glass transition point T_g for DSC was defined as the inflection point in the DSC curve.

2.3 Dynamic mechanical analysis

The temperature dependent properties of BMC-G and PMMA composites were examined using Dynamic Mechanical Analysis (DMA) (Patra et al., 2020). DMA was performed on 3 samples from each of the groups. A bar (2 mm × 3 mm x 15 mm) was placed into a 3-point bending fixture of a RSA G2 DMA machine (TA Instruments). A small oscillating displacement with a peak of 15 μm was applied at a frequency of 15 Hz as the sample was heated from 0°C to 150°C. The storage modulus (ability to store energy elastically), loss modulus (ability to dissipate energy), and tan delta (ratio of loss and storage modulus) were calculated at each temperature.

2.4 Disc diffusion assay

All of the constructs were placed in 48-well plates filled with 1 mL of normal saline warmed to 37°C to replicate body conditions. The concentration of the gentamicin or vancomycin eluted into the saline was sampled at days 1, 2, 3, 4, 5, 7, 10, 15, 20 and 30. At each time point, the saline surrounding the reservoir was collected and replaced with fresh saline to maintain sink diffusion conditions. All samples were stored at −20°C until all time points had been collected. The samples were thawed at 4°C for a disc diffusion assay (Balouiri et al., 2016). An overnight culture of *Escherichia coli* (EC) (ATCC 25922) for the gentamicin samples and *Staphylococcus Aureus* (SA) (ATCC 29213) for the vancomycin samples was prepared in 3 mL of sterile Muller Hinton II Broth (MilliporeSigma) (Minogue et al., 2014; Soni et al., 2015). The bacterial solution was diluted to have an optical density of 0.50 at 600 nm measured with an Ultraspec 10 cell density meter (Biochrom). This corresponded to 5×10^7 Colony Forming Units (CFU)/mL for EC and 1×10^9 CFU/mL for SA. 40 µL of EC or 20 µL of SA were spread evenly with an inoculation loop on 90 mm diameter Petri dishes filled with 30 mL of Muller Hinton agar (Difco). Next, five 6 mm Whatman antibiotic assay discs were placed onto each agar plate and loaded with 20 µL of thawed recovered saline. The agar plates were incubated overnight at 37°C and imaged after 16 h. Using ImageJ software (FIJI), the Zone of Inhibition (ZOI) or the diameter of the circle around the disc where bacteria was not able to grow, was measured. Saline samples with known concentrations of antibiotics were tested to produce a standard curve and allow for the concentration of antibiotic to be calculated from the ZOI. The cumulative release was calculated by multiplying the measured concentration of antibiotic by the volume of the recovered saline (1 mL) and adding to the cumulative release from the prior timepoint. The 30-day time point was chosen after preliminary experiments with PMMA mixed with clinically used amounts of antibiotics demonstrated that the drug concentration in those samples was too low to produce a measurable ZOI using the method described above.

2.5 Compression testing

The compressive properties of the BMC and PMMA composite were evaluated by compressing test cylinders with a height of 12 mm and a diameter of 6 mm from each group in accordance with ISO 5833 (ISO - ISO 5833, 2022). Five samples from each composite group were tested before and after the 30-day elution. Each test cylinder was polished and measured with calipers before being placed between compression platens of a TR nano uniaxial test frame (Test Resources). The samples were compressed at a rate of 20 mm/min. Compressive stress was calculated from the load that was measured using a 25 kN load cell. Compressive strain was calculated from the vertical displacement of the crosshead. The yield strength was calculated using the 0.2% offset method (Morgan and Keaveny, 2001).

2.6 Scanning electron microscopy

The surface features of the composite samples after the 30-day elution were examined using scanning electron microscopy (SEM). The samples were dried and placed inside a Hitachi TM3030Plus Tabletop so the long axis of the cylinder faced the electron source. Electrons were accelerated at 15 kV at the samples and secondary electrons were detected to produce an image at ×100 magnification.

2.7 Statistical analysis

Results were reported as averages with one standard error. One way ANOVA was used to compare the average T_g values. R^2 coefficients were calculated to assess the quality of the standard curves relating the size of the ZOI to the concentration of antibiotics. The standard deviation for the cumulative release plots was calculated by summing the variance measured at the time point and all the previous time points, and then taking the square root of the cumulative variance. A multivariate linear regression model was used to assess the independent effects of drug concentration and the 30-day elution on the compressive properties of the BMC and PMMA composites. All statistical analysis was conducted with RStudio.

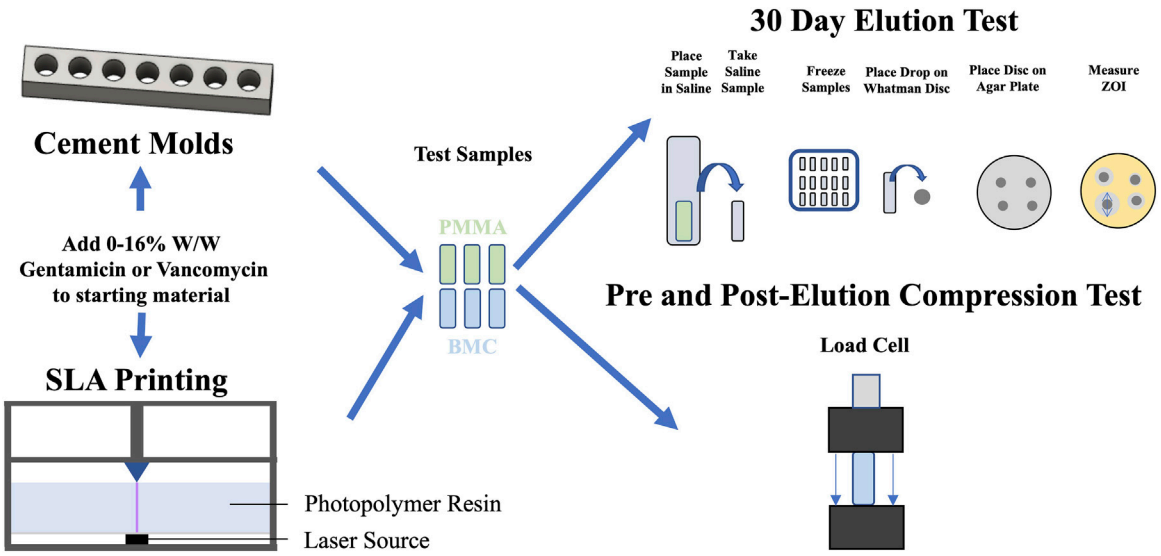

FIGURE 1
Schematic overview of the evaluation of elution and compressive mechanical properties for PMMA (green) and BMC (blue) composites that contained antibiotics. PMMA composite cylinders were fabricated using molds, while BMC cylinders were 3D-printed. Each iteration of the composites underwent a 30-day elution study and compressive mechanical testing, conducted both before and after the elution period.

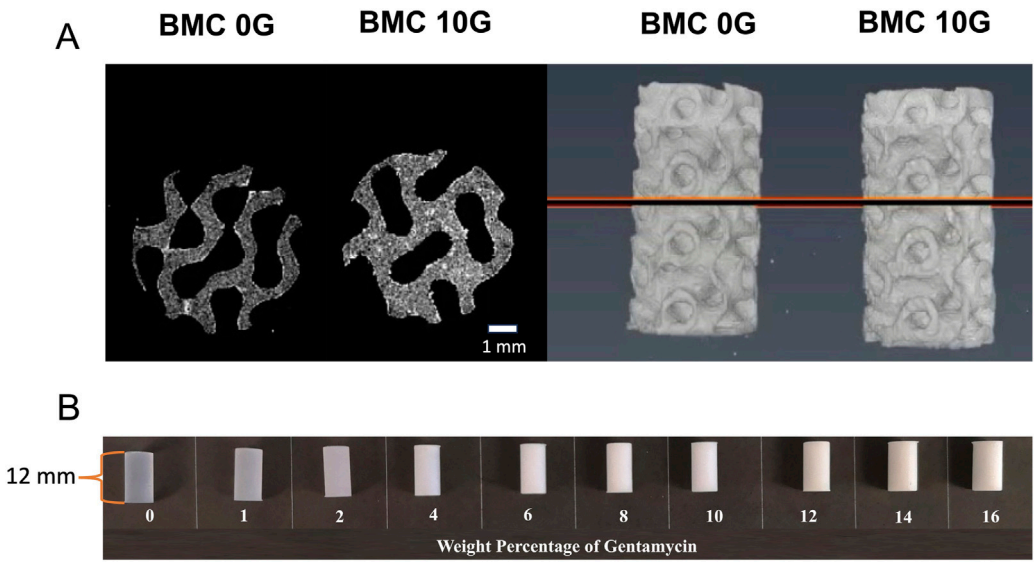

FIGURE 2
(A) Micro CT images of a gyroid lattice cylinder printed with BMC resin loaded with and without 10% gentamicin demonstrating that the addition of antibiotic does not prevent the printing of complex geometries. **(B)** BMC cylinders printed from resin loaded with increasing concentrations of gentamicin demonstrating the range of antibiotics that can be loaded into the composite structures.

3 Results

3.1 Range of antibiotic doping

The doped resin was still able to selectively polymerize the resin with the same print settings to form complex structures like a gyroid lattice. (Figure 2A). As gentamicin or vancomycin was added to the BMC resin, the printed samples went from a translucent appearance to a white opaque appearance (Figure 2B). Up to 16% gentamicin or 10% vancomycin could be added to the BMC resin before the prints started to fail.

3.2 Differential scanning calorimetry

DSC was used to measure the T_g of the BMC (Figure 3A) and PMMA (Figure 3B) composites. The BMC composites had T_g

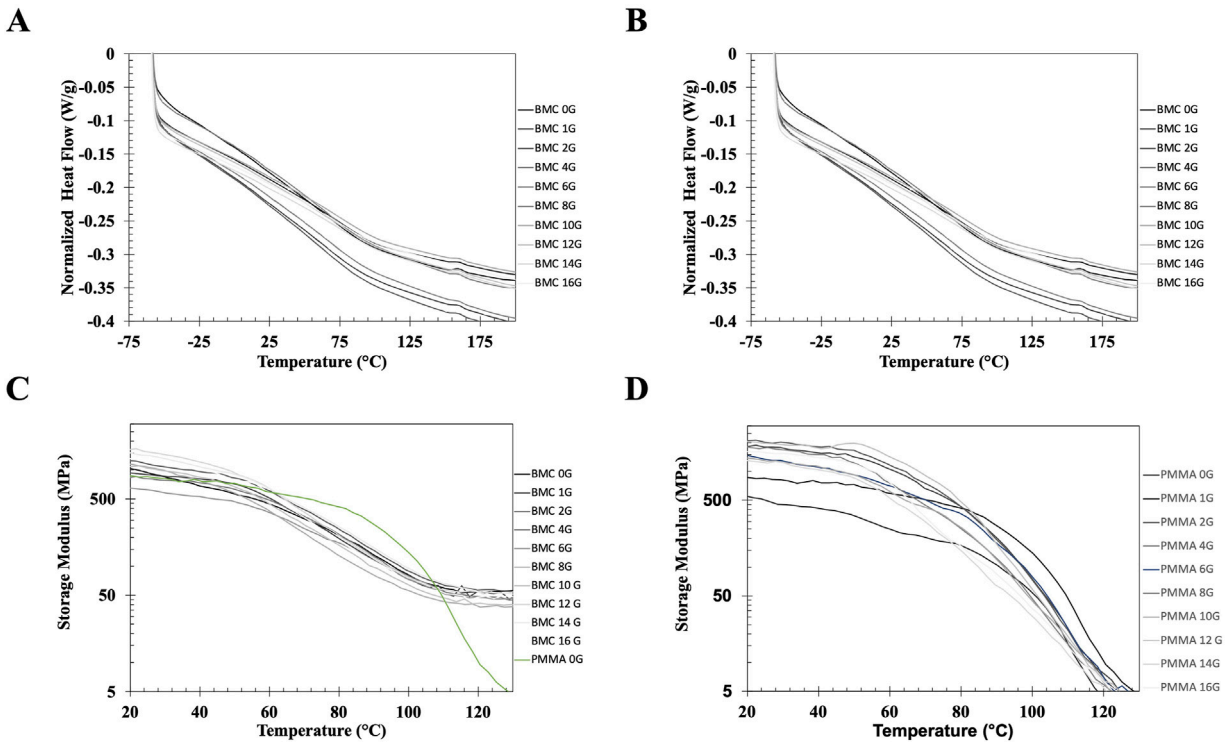

FIGURE 3
(A, B) Representative DSC heating curves of samples printed with BMC **(A)** and PMMA bone cement **(B)** doped with increasing concentrations of gentamicin. The DCS curves demonstrate that adding a relatively small molecule to BMC or PMMA do not alter the glass transition of the polymer. **(C, D)** Representative DMA curves showing the storage modulus **(C)** BMC and PMMA bone cement **(D)** loaded with increasing amounts of gentamicin and PMMA bone cement from 0°C to 150°C. The green curve in 3C represents PMMA without any antibiotics on the same curve as the BMC curves to highlight the difference between the DMA properties. The DMA curves demonstrate that the BMC composite behave as a thermoset while the PMMA composite behave as a thermoplastic.

values of 65.0 ± 1.5°C and the PMMA composite had T_g values of 102.3 ± 2.2°C. The addition of gentamicin did not alter the T_g of the BMC composites ($p = 0.941$) or the PMMA composites ($p = 0.251$).

3.3 Dynamic mechanical analysis

The storage modulus, E, for each of the BMC-G groups and PMMA bone cement was plotted from 0°C – 150°C on a logarithmic scale (Figure 3C). There is overlap between the BMC-G concentrations, suggesting that the addition of antibiotics does not change the mechanical properties at small displacements over a wide range of temperatures. In all the BMC-G plots, the storage modulus decreases modestly at 60°C and plateaus at 150°C. In contrast, the storage modulus of PMMA bone cement starts to decrease significantly at 80°C, and continues to decrease at higher temperatures. The BMC plots are consistent with a thermoset while the PMMA plots are consistent with a thermoplastic.

3.4 Compression

The representative stress-strain curves for the BMC and PMMA composites are shown in Figure 4. None of the samples fractured before 10% strain, but they underwent barreling. In general, the stress-strain curves for BMC composites did not significantly vary with the increased percentage of antibiotics. A notable exception included BMC 16G post-elution samples that were significantly less stiff and had a lower strength than the rest of the BMC G composite post-elution. Another exception was that the addition of any amount of vancomycin significantly lowered the compressive strength of the samples. The different groups of PMMA composite varied more in general compared to the BMC curves. Trends were further analyzed by plotting the modulus, yield strength, and ultimate strength as a function of drug concentration for each type of composite (Figure 5). The BMC lines (black) did not change as much with increasing drug concentration as the PMMA lines (gray). Most of the samples got stronger and stiffer after the 30-day elution (dashed lines) compared to before the 30-day elution (solid lines) with the exception of the PMMA samples with over 8% antibiotics. The effect of drug concentration and the 30-day elution were quantified with a multivariate linear regression model (Table 1). There was a statistically significant decrease in modulus, yield strength, and ultimate strength associated with doping PMMA composites with additional antibiotics. In contrast, the addition of antibiotics did not statistically alter the modulus or yield strength for the BMC composites. There was a 0.25 MPa decrease in ultimate strength associated with each

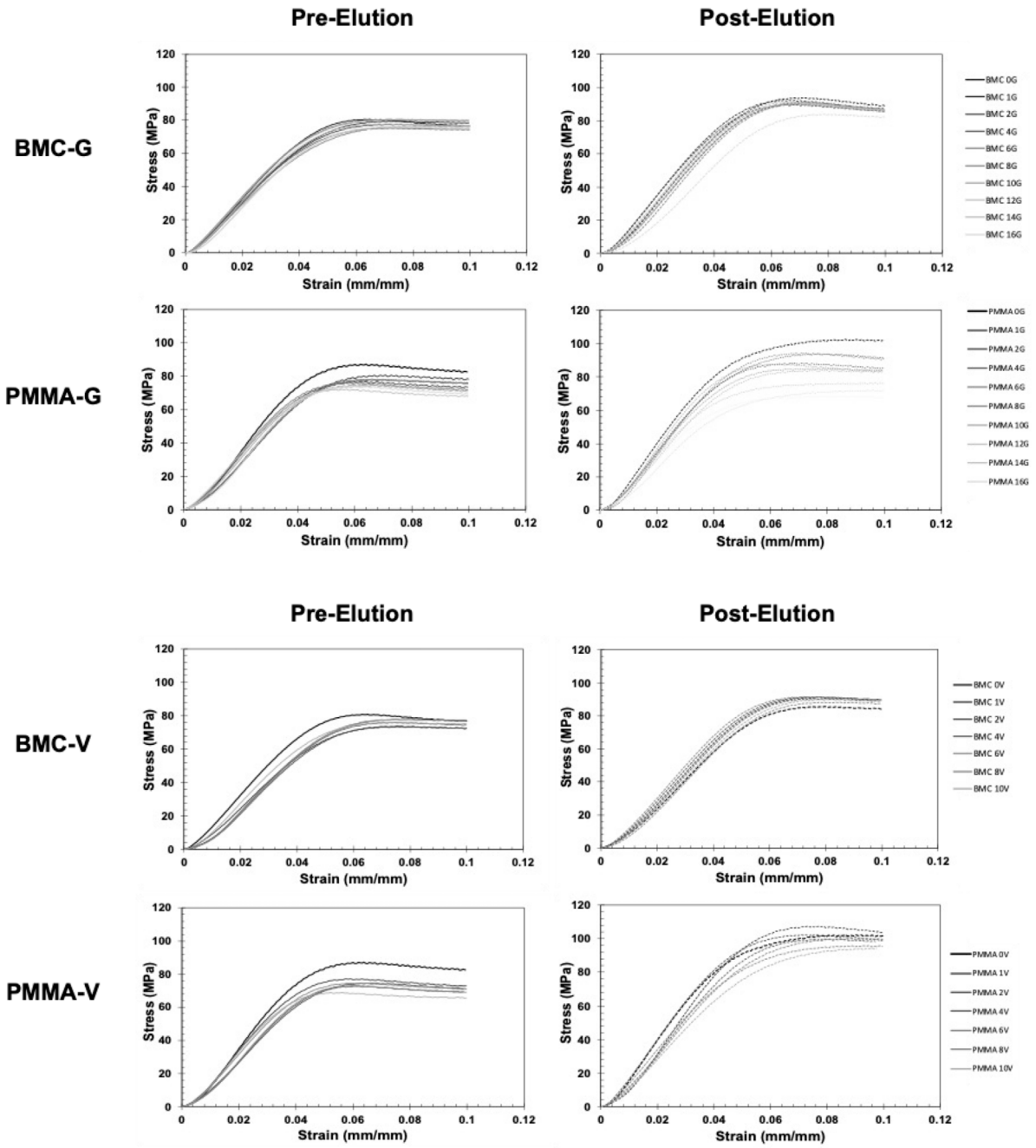

FIGURE 4
Representative stress-strain curves of antibiotic BMC and PMMA composites loaded in compression. Samples were tested before (left) and after (right) a 30-day elution. Black curves represent control samples without antibiotics. The lighter gray curves represent samples with increasing weight percentage of antibiotic.

percent increase of gentamicin. The same increase in gentamicin was associated with a 1.17 MPa decrease in ultimate strength in the PMMA composites.

3.5 Antibiotic elution properties

The standard curve demonstrated that ZOI measurements could be used to accurately measure the concentration of the antibiotics from 8 μg/mL to 10,000 μg/mL (Supplementary Figure S1). The R^2 values were 0.99 for both the gentamicin and vancomycin standard curve. The concentration of antibiotic that eluted between each timepoint is shown in Figure 6 on a logarithmic scale. There was a measurable ZOI from most samples over the 30-day elution with the exception of BMC-G composites with less than 8% gentamicin and PMMA-G composite with less than 4% gentamicin. Overall, samples released more antibiotics at the early time points.

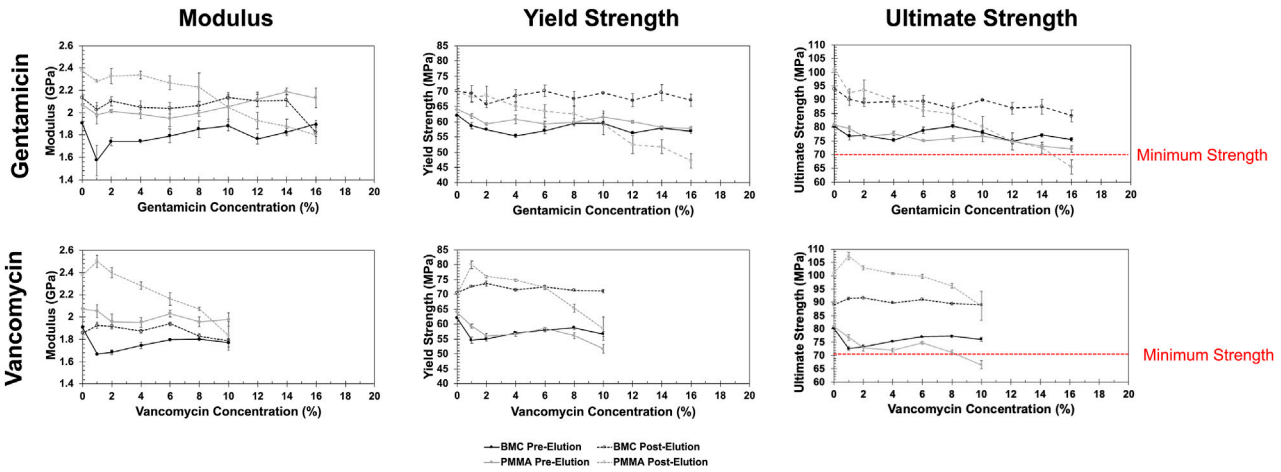

FIGURE 5
Summary plots of how the calculated compressive properties including modulus (left), yields strength (middle) and ultimate strength (right) changed with each concentration of gentamicin (top) and vancomycin (bottom) for the BMC (black) and PMMA (gray) composites. Data from dried samples tested before (solid) and after (dashed) a 30-day elution.

TABLE 1 A summary of a multivariate linear regression model that assessed the independent association between either drug concentration or the 30-day elution on the compressive properties of the BMC and PMMA composites.

Modulus (MPa)								
	BMC-G		PMMA-G		BMC-V		PMMA-V	
	Δ MPa	p Value	Δ MPa	p Value	Δ MPa	p Value	Δ MPa	p Value
Change Associated with a 1% Increase in Antibiotic Concentration	0.87	0.75	−13.33	<0.001	−6.93	0.37	−31.99	0.002
Change Associated with a 30 Days of Elution	261.69	<0.001	97.75	0.02	159.14	0.004	286.95	<0.001
Yield Strength (MPa)								
	BMC-G		PMMA-G		BMC-V		PMMA-V	
	Δ MPa	p Value	Δ MPa	p Value	Δ MPa	p Value	Δ MPa	p Value
Change Associated with a 1% Increase in Antibiotic Concentration	−0.09	0.18	−0.81	<0.001	−0.16	0.53	−1.13	<0.001
Change Associated with a 30 Days of Elution	10.40	<0.001	0.62	0.56	16.08	<0.001	15.14	<0.001
Ultimate Strength (MPa)								
	BMC-G		PMMA-G		BMC-V		PMMA-V	
	Δ MPa	p Value	Δ MPa	p Value	Δ MPa	p Value	Δ MPa	p Value
Change Associated with a 1% Increase in Antibiotic Concentration	−0.25	<0.001	−1.17	<0.001	−0.17	0.60	−1.17	0.001
Change Associated with a 30 Days of Elution	11.31	<0.001	7.87	<0.001	16.43	<0.001	28.01	<0.001

Some curves have an increased measured concentration after day 5 (Figure 6). This is due to the time points being spread out, giving the samples more time to elute antibiotics. There was more antibiotic eluted from the PMMA composites and from samples with a higher concentration of antibiotics (Figure 7). Both PMMA and BMC samples doped with gentamicin were still bactericidal when placed directly on a bacterial Petri dish after the 30-day elution. (Figure 8). The undoped controls were not able to prevent bacteria from growing up to the surface. The BMC 1G samples prevented bacteria growth within a small area around the cylinder. All other composites produced an oval-shaped zone of inhibition around the cylinder.

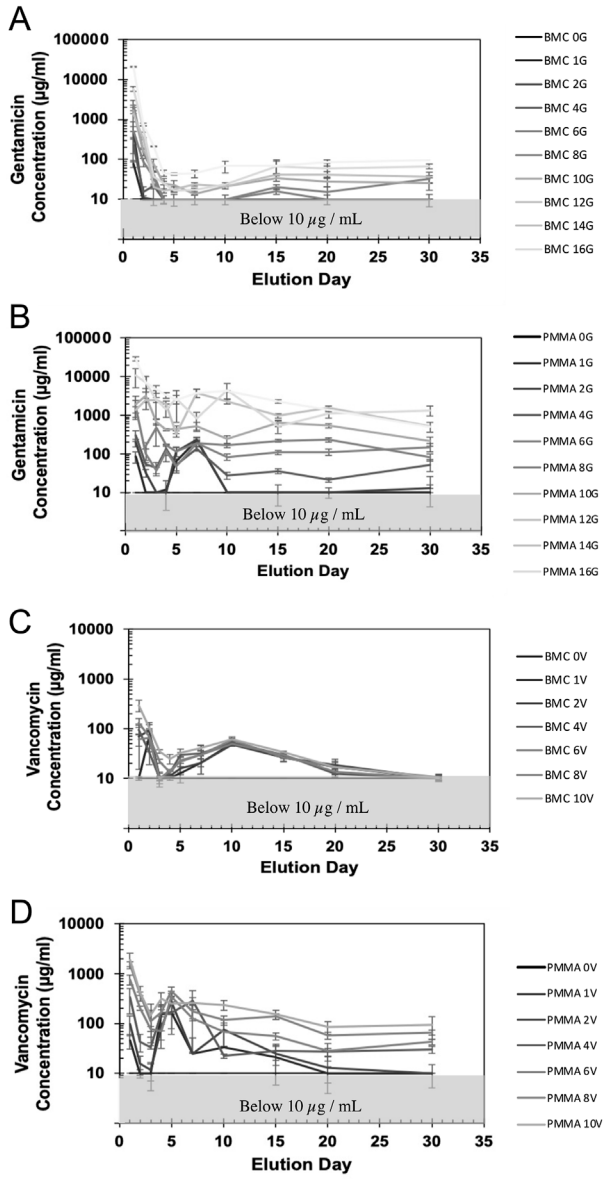

FIGURE 6
The concentration of gentamicin **(A, B)** and vancomycin **(C, D)** measured in the recovered saline surrounding the BMC **(A, C)** or the PMMA **(B, D)** composites. Concentrations below 10 µg/mL were not able to be accurately measured by the disc diffusion assay.

3.6 Scanning electron microscopy

SEM imaging of the samples after the 30-day elution highlight differences in the surface morphology. (Figure 9). Dried salt crystals from the saline can be seen on the surface. The BMC samples are relatively free from defects. In contrast, there are 50–100 µm diameter craters on the PMMA samples.

4 Discussion

This study demonstrated that a biocompatible 3D printing resin can be loaded with high concentrations of antibiotics. The mechanical and antibiotic elution properties of the composite were then compared to the standard of care for PJI, PMMA-based bone cement composite spacers. BMC could be doped with up to 16% gentamicin and 10% vancomycin before the light-based 3D prints failed from the opaque powder scattering the laser light. The addition of the antibiotic powder increases the viscosity of the resins and absorbs the laser light (λ = 365 nm), leading to a less efficient polymerization reaction and network formation. However, DSC measurements indicated that gentamicin incorporation did not alter the network structure of the BMC or PMMA. The T_g for both polymers did not significantly change with gentamicin. T_g is reflective of polymer chain mobility, which can be altered by the molecular weight, inter- and intramolecular forces, plasticizers, crosslinks, and crystallization (Schut et al., 2007; Painter and Coleman, 2019).

Any material used to treat PJI should release therapeutic levels of antibiotics or at the very least be able to prevent bacterial colonization on the implant. The minimal inhibitory concentration is typically used as a benchmark for drug elution in PMMA (Duey et al., 2012; Moore et al., 2021; Lunz et al., 2022). It is important to note the reported MICs for an antibiotic are specific to a strain of bacteria *in vitro* (Kowalska-Krochmal and Dudek-Wicher, 2021). The MIC represents the minimum concentration of antibiotics reported in µg/mL that prevents visible growth of bacteria. The MIC of gentamicin for EC strain ATCC 25922, the strain used in this study, is reported to be 0.12–1 µg/mL (Fass and Barnishan, 1979). The MIC for vancomycin for SA strain 29213 used in the study is reported to be 1 µg/mL, while the MIC of vancomycin-susceptible SA from clinical isolates ranges from 0.5–1 µg/mL (Entenza et al., 2014). The elution samples in this study from BMC-G samples with over 6% gentamicin and PMMA-G samples with over 2% gentamicin contained over 10 µg/mL of gentamicin over the course of 30 days. All of the doped BMC-V samples and all the PMMA-V samples except for PMMA 1V contained vancomycin levels above the MIC for SA strain 29213. It is important to note that even when the measured drug concentration fell below the detectable limit of the disc diffusion assay (Figure 6), a measurable bactericidal effect was observed when the gentamicin composite was placed directly on the bacterial plate (Figure 8). Past studies have shown that materials like PMMA can provide a surface for bacterial colonization once the embedded antibiotic falls below the MIC (Vugt et al., 2019). However, the results of this study suggest that even after active antibiotic elution has concluded for both BMC and PMMA composites, the embedded antibiotics still protect the surface of material from bacterial colonization (Xi et al., 2021). In comparison to the BMC composite, the PMMA composite eluted significantly more drug, and the quantity of the drug release depended on the amount of drug added to the original sample. The diminished total release in antibiotics in the BMC samples reduce both the bactericidal potential as well as the risk of systemic side effects from the antibiotics. There was also a stark difference in the elution profile between antibiotics. The gentamicin sample released an order of magnitude more drug than the vancomycin samples. Both drugs have a similar solubility in water, 50 mg/mL for gentamicin and >100 mg/mL for vancomycin (Gentamicin sulfate USP, 2023; Vancomycin hydrochloride, 2023; Della Porta et al., 2016). However, vancomycin is a much larger molecule with a

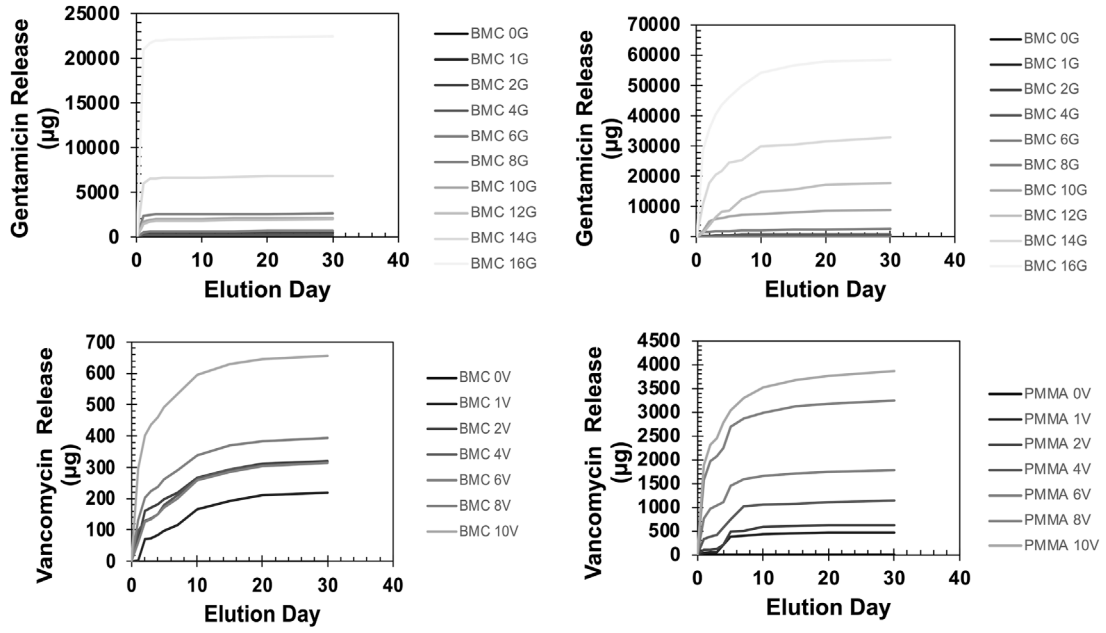

FIGURE 7
The cumulative release of gentamicin (top) and vancomycin (bottom) in the recovered saline sounding the BMC (left) or the PMMA (right) composites over a 30-day elution. Error bars represent standard deviation.

molecular weight of 1449.3 g/mol compared to 449.5–477.6 g/mol for gentamicin (Isoherranen and Soback, 2000; Ferraris et al., 2010) The small gentamicin may be able to diffuse more easily through the polymer chain than the vancomycin. As with any application using antibiotics, antibiotic stewardship must be taken into account (Shrestha et al., 2023). Both the BMC and the PMMA composites currently in use have the potential risk of accelerating antibiotic resistance once the drug concentration falls below the MIC (Hickok et al., 2018). The increased risk of antibiotic resistance must be carefully weighed against decreased risk of systemic side effects and the potential to incorporate the most effective antibiotic into the polymer based on susceptibility studies.

In addition to releasing antibiotics, materials used as spacers to treat PJI need to be able to withstand loads typical of a partially weight-bearing patient. Compressive properties of the BMC and PMMA composites were affected by both the 30-day elution period and the starting concentration of antibiotic in the composite. The compressive modulus and the ultimate compressive strength significantly increased after a 30-day elution for the BMC and PMMA composites. The water likely leached uncured monomers that acted as plasticizers within the crosslinked polymer network (Seo et al., 2007; Aldhafyan et al., 2022). The compressive properties of PMMA composites were negatively impacted by the antibiotic concentration. The BMC composites were relatively unaffected by increasing antibiotic concentration. The results are consistent with previous studies that showed PMMA-loaded spacers reached a maximum antibiotic mass fraction of 6.5% before mechanical properties were reduced and too weak for clinical use (Pelletier et al., 2009). The results of the mechanical testing at the two timepoints in the saline solution demonstrate that exposure to an aqueous environment can potentially alter the mechanical properties of both BMC and PMMA composites. For future applications of these composites, the findings highlight the need to test the mechanical properties at multiple timepoints throughout the intended use time of the materials to ensure appropriate safety during the life of the material.

The difference in elution and compressive properties between BMC and PMMA can be explained by understanding the polymer networks. BMC is a thermoset, where the polymer chains are secured by chemical crosslinks. In contrast, PMMA is a thermoplastic, where the polymer chains are held together by non-covalent intermolecular forces (Yan et al., 2020). The difference in the polymer networks is best highlighted in the DMA plots (Figure 3C). The storage modulus of BMC plateaus after the glass transition, while the storage modulus continues to decrease with higher temperatures in PMMA. The crosslinked network of BMC allows for the fabrication of precise objects during printing, but does not allow for additives like antibiotics to as easily diffuse into the surrounding saline compared to an uncrosslinked PMMA polymer. The same crosslinks that limit the magnitude of drug elution made the compressive properties resistant to the increased concentration of antibiotics.

The optimal composite is dependent on the clinical situation. 3D printing a BMC composite could be advantageous if a surgeon needs a patient-specific implant. This can occur if the patient is not a standard size, the patient is undergoing a complicated revision surgery, or a surgeon needs to adjust the offset – either increasing it to reduce the joint reaction force or decreasing it if he or she is worried about the bone-implant interface (Rüdiger et al., 2017). In contrast, a PMMA spacer would be advantageous if a surgeon is not able to completely debride the infected tissue because of the increased antibiotic delivery, or if the patient is non-weight bearing and the mechanical properties are less consequential.

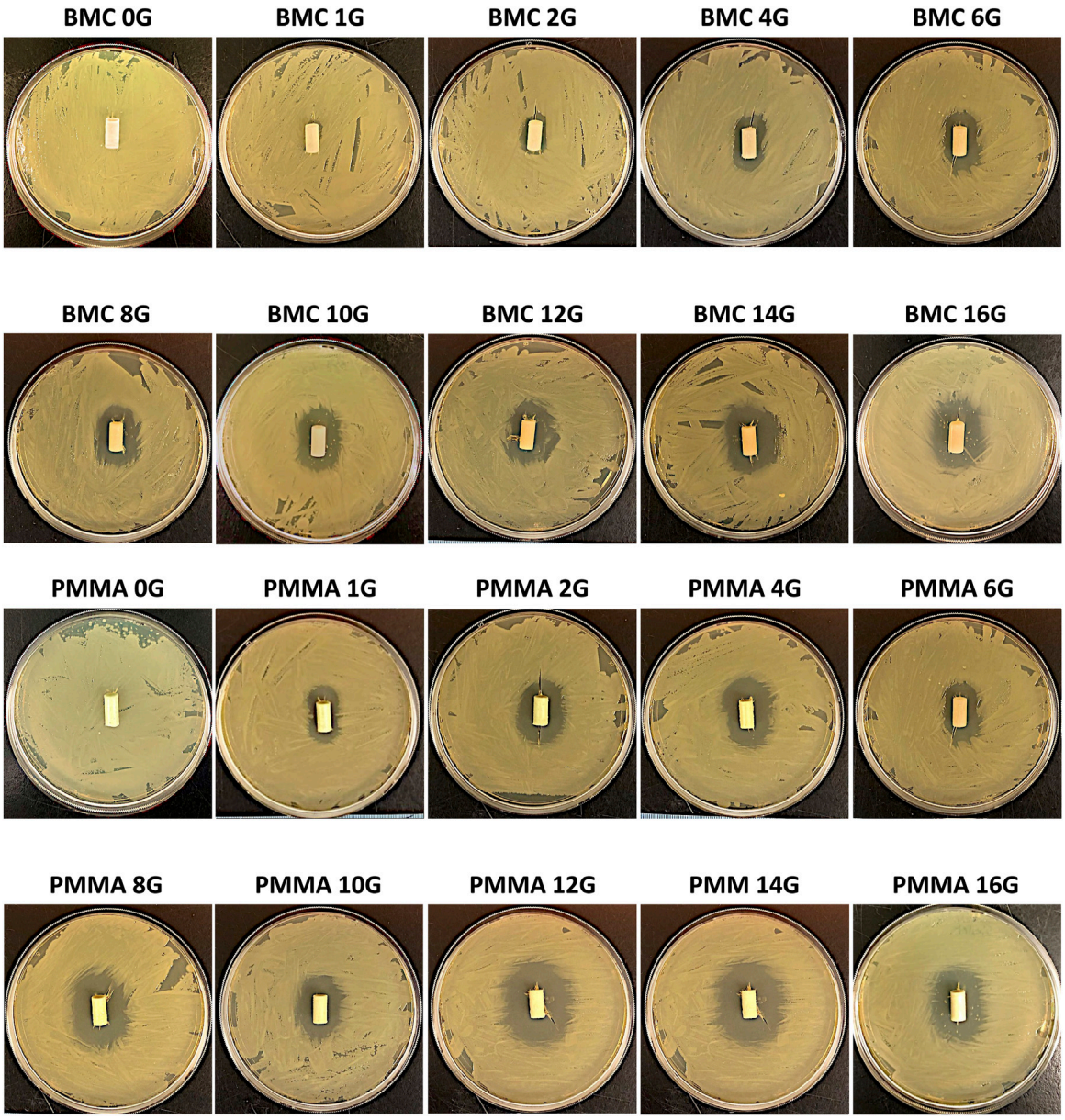

FIGURE 8
The bactericidal effects of the BMC-G (top) and PMMA-G (bottom) after the 30-day elution. Sample containing gentamicin-killed bacteria around the surface. Bacteria were able to grow up to the surface in the negative control without any antibiotics.

This study has inherent limitations that need to be considered. First, saline was used to simulate the fluid surrounding a temporary spacer. The actual synovial fluid and surrounding fluid is more complex and includes white blood cells and cytokines that could impact the material properties over time (Zmistowski et al., 2012; Prince et al., 2020). Second, antibiotic levels were measured with a disc diffusion assay, which is not as precise as other methods like HPLC, but have the advantage of verifying the biological activity of the eluted antibiotic (Webb et al., 2013; Al Thaher et al., 2021). Finally, the PMMA composite was mixed by hand and not by vacuum mixing, which could impact how pores develop in the composite (Macaulay et al., 2002; Messick et al., 2007). This study focused on gentamicin and vancomycin, but other antimicrobials are used to treat PJI, including antifungals, and combinations of drugs, and should be tested in BMC and PMMA composites (Nace et al., 2019). Benchtop models allow scientists to efficiently screen several iterations of composites. While the individual components of the BMC composite (BMC resin and antibiotics) have been shown to be biocompatible, the composite has not undergone extensive toxicities studies. Before translation to patients can take place, any new approach to treating PJI needs to be tested in an infected animal model where the ability to treat the PJI can be accurately evaluated and failure modes, including fracture of the implants, joint dislocations, and drug toxicity, can be monitored under physiological conditions (Stavrakis et al., 2013; Jie et al., 2019).

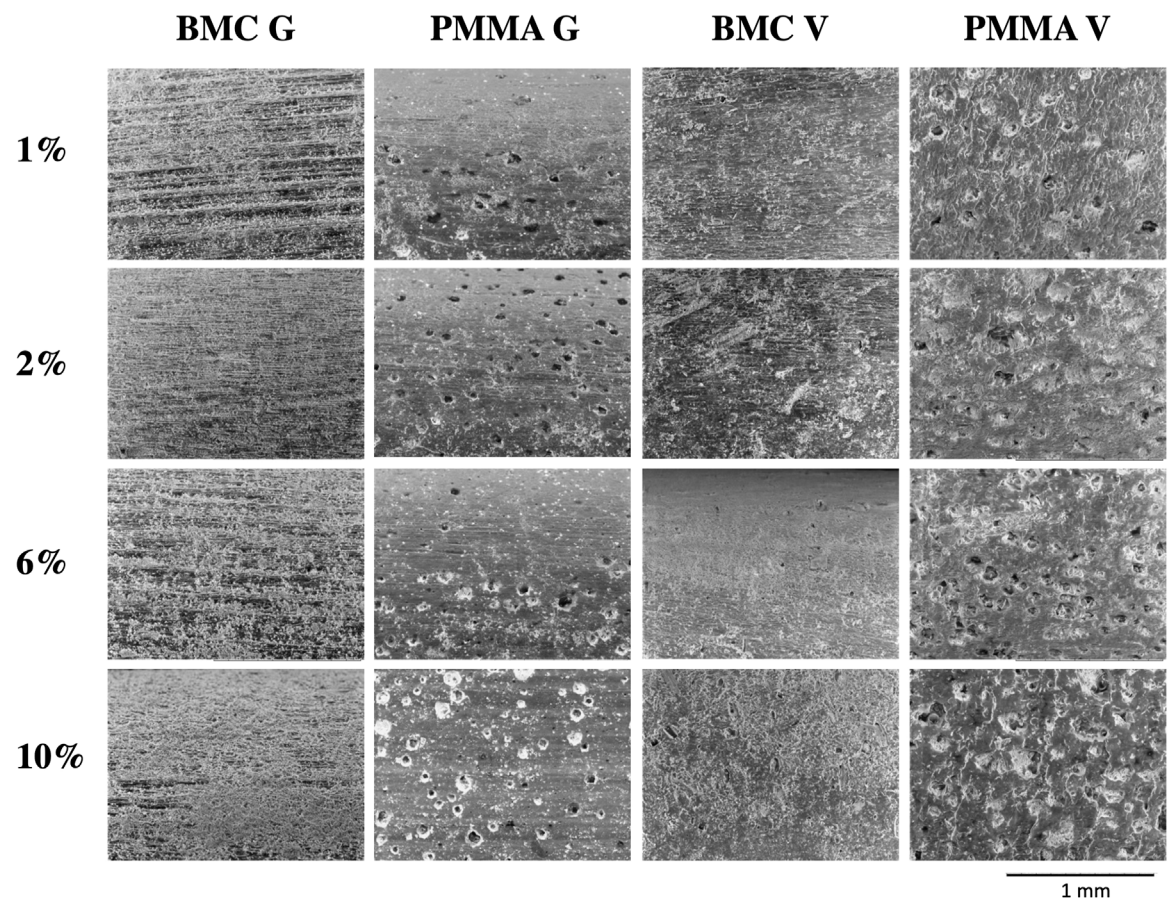

FIGURE 9
SEM images of the surface of BMC and PMMA composites after the 30-day elution.

In conclusion, this study demonstrated a novel method of fabrication for weight-bearing composites that can release antibiotics. BMC is a photopolymerized resin that can be loaded with up to 16% gentamicin or 10% vancomycin. As a thermoset, BMC more effectively maintains its compressive properties at greater antibiotic loads. However, its crosslinked structure limits the amount of drug that can be released compared to the PMMA standard of care. The characterization of BMC and PMMA composites provides important preclinical data that can aid in the development of improved treatments for PJIs as well as other infections.

Data availability statement

The raw data supporting the conclusions of this article will be made available by the authors, without undue reservation.

Ethics statement

Ethical approval was not required for the studies on animals in accordance with the local legislation and institutional requirements because only commercially available established cell lines were used.

Author contributions

BA: Conceptualization, Data curation, Formal Analysis, Investigation, Methodology, Visualization, Writing – original draft, Writing – review and editing, Validation. HG: Data curation, Formal Analysis, Investigation, Writing – original draft, Writing – review and editing. RS: Data curation, Formal Analysis, Investigation, Visualization, Writing – review and editing. MN: Formal Analysis, Investigation, Methodology, Visualization, Writing – review and editing. NA: Formal Analysis, Investigation, Writing – review and editing. CK: Conceptualization, Formal Analysis, Methodology, Writing – review and editing. NS: Formal Analysis, Investigation, Writing – review and editing. MB: Conceptualization, Formal Analysis, Methodology, Resources, Supervision, Writing – review and editing, Visualization. JT: Formal Analysis, Investigation, Methodology, Resources, Supervision, Writing – review and editing, Visualization. SA: Conceptualization, Formal Analysis, Methodology, Resources, Supervision, Writing – review and editing. KG: Writing – review and editing, Conceptualization, Formal Analysis, Funding acquisition, Methodology, Project administration, Resources, Supervision, Visualization.

Funding

The author(s) declare that no financial support was received for the research and/or publication of this article.

Acknowledgments

This work was performed in part at the Duke University Shared Materials Instrumentation Facility (SMIF), a member of the North Carolina Research Triangle Nanotechnology Network (RTNN), which is supported by the National Science Foundation (Grant ECCS-1542015) as part of the National Nanotechnology Coordinated Infrastructure (NNCI). Duke Innovation Co-Lab provided space, instruments and expertise that supported research in this publication. We acknowledge Esme Park for her contributions to the data acquisition and figure generation that supported this manuscript.

Conflict of interest

Authors BA, CK and KG have equity in Reselute. The remaining authors declare that the research was conducted in the absence of any commercial or financial relationships that could be construed as a potential conflict of interest.

Publisher's note

All claims expressed in this article are solely those of the authors and do not necessarily represent those of their affiliated organizations, or those of the publisher, the editors and the reviewers. Any product that may be evaluated in this article, or claim that may be made by its manufacturer, is not guaranteed or endorsed by the publisher.

Supplementary material

The Supplementary Material for this article can be found online at: https://www.frontiersin.org/articles/10.3389/fbiom.2025.1394166/full#supplementary-material

SUPPLEMENTAL FIGURE S1
Standard curve relating the known concentration of gentamicin (top) and vancomycin (bottom) to a measured ZOI.

References

Aldhafyan, M., Silikas, N., and Watts, D. C. (2022). Influence of curing modes on monomer elution, sorption and solubility of dual-cure resin-cements. *Dent. Mater.* 38, 978–988. doi:10.1016/J.DENTAL.2022.03.004

Al Thaher, Y., Alotaibi, H. F., Yang, L., and Prokopovich, P. (2021). PMMA bone cement containing long releasing silica-based chlorhexidine nanocarriers. *PLoS One* 16, e0257947. doi:10.1371/JOURNAL.PONE.0257947

Anguita-Alonso, P., Hanssen, A. D., Osmon, D. R., Trampuz, A., Steckelberg, J. M., and Patel, R. (2005). High rate of aminoglycoside resistance among staphylococci causing prosthetic joint infection. *Clin. Orthop. Relat. Res.* 439, 43–47. doi:10.1097/01.BLO.0000182394.39601.9D

Balouiri, M., Sadiki, M., and Ibnsouda, S. K. (2016). Methods for *in vitro* evaluating antimicrobial activity: a review. *J. Pharm. Anal.* 6, 71–79. doi:10.1016/J.JPHA.2015.11.005

BioMed Clear Resin (2024). *Formlabs*. Available online at: https://formlabs.com/store/materials/biomed-clear-resin/ (Accessed April 17, 2024).

Carli, A. V., Sethuraman, A. S., Bhimani, S. J., Ross, F. P., and Bostrom, M. P. G. (2018). Selected heat-sensitive antibiotics are not inactivated during polymethylmethacrylate curing and can Be used in cement spacers for periprosthetic joint infection. *J. Arthroplasty* 33, 1930–1935. doi:10.1016/j.arth.2018.01.034

Charette, R. S., and Melnic, C. M. (2018). Two-stage revision arthroplasty for the treatment of prosthetic joint infection. *Curr. Rev. Musculoskelet. Med.* 11, 332–340. doi:10.1007/S12178-018-9495-Y

Chen, L., Tang, Y., Zhao, K., Zha, X., Liu, J., Bai, H., et al. (2019). Fabrication of the antibiotic-releasing gelatin/PMMA bone cement. *Colloids Surf. B Biointerfaces* 183, 110448. doi:10.1016/J.COLSURFB.2019.110448

Della Porta, G., Campardelli, R., Cricchio, V., Oliva, F., Maffulli, N., and Reverchon, E. (2016). Injectable PLGA/Hydroxyapatite/Chitosan microcapsules produced by supercritical emulsion extraction technology: an *in vitro* study on teriparatide/gentamicin controlled release. *J. Pharm. Sci.* 105, 2164–2172. doi:10.1016/J.XPHS.2016.05.002

Duey, R. E., Chong, A. C. M., McQueen, D. A., Womack, J. L., Song, Z., Steinberger, T. A., et al. (2012). Mechanical properties and elution characteristics of polymethylmethacrylate bone cement impregnated with antibiotics for various surface area and volume constructs. *Iowa Orthop. J.* 32, 104–115.

Eckers, F., Laux, C. J., Schaller, S., Berli, M., Achermann, Y., and Fucentese, S. F. (2021). Risk factor analysis for above-knee amputation in patients with periprosthetic joint infection of the knee: a case-control study. *BMC Musculoskelet. Disord. 2021* 22 (22), 884–14. doi:10.1186/S12891-021-04757-W

Entenza, J. M., Bétrisey, B., Manuel, O., Giddey, M., Sakwinska, O., Laurent, F., et al. (2014). Rapid detection of *Staphylococcus aureus* strains with reduced susceptibility to vancomycin by isothermal microcalorimetry. *J. Clin. Microbiol.* 52, 180–186. doi:10.1128/JCM.01820-13

Fass, R. J., and Barnishan, J. (1979). Minimal inhibitory concentrations of 34 antimicrobial agents for control strains *Escherichia coli* ATCC 25922 and *Pseudomonas aeruginosa* ATCC 27853. *Antimicrob. Agents Chemother.* 16, 622–624. doi:10.1128/AAC.16.5.622

Ferraris, S., Miola, M., Bistolfi, A., Fucale, G., Crova, M., Massé, A., et al. (2010). *In vitro* comparison between commercially and manually mixed antibiotic-loaded bone cements. *J. Appl. Biomater. Biomech.* 8, 166–174. doi:10.5301/JABB.2010.6068

Gbejuade, H. O., Lovering, A. M., and Webb, J. C. (2015). The role of microbial biofilms in prosthetic joint infections. *Acta Orthop.* 86, 147–158. doi:10.3109/17453674.2014.966290

Gentamicin sulfate USP (2023). Available online at: https://us.vwr.com/store/product/14513840/gentamicin-sulfate-usp (Accessed March 6, 2023).

Gill, P., Moghadam, T. T., and Ranjbar, B. (2010). Differential scanning calorimetry techniques: applications in biology and nanoscience. *J. Biomol. Tech.* 21, 167–193.

Hickok, N. J., Shapiro, I. M., and Chen, A. F. (2018). The impact of incorporating antimicrobials into implant surfaces. *J. Dent. Res.* 97, 14–22. doi:10.1177/0022034517731768

Isoherranen, N., and Soback, S. (2000). Determination of gentamicin after trimethylsilylimidazole and trifluoroacetic anhydride derivatization using gas chromatography and negative ion chemical ionization ion trap mass spectrometry. *Analyst* 125, 1573–1576. doi:10.1039/B003710I

ISO - ISO 5833 (2022). 2002 - implants for surgery — acrylic resin cements. Available online at: https://www.iso.org/standard/30980.html (Accessed August 30, 2022).

Jie, K., Deng, P., Cao, H., Feng, W., Chen, J., and Zeng, Y. (2019). Prosthesis design of animal models of periprosthetic joint infection following total knee arthroplasty: a systematic review. *PLoS One* 14, e0223402. doi:10.1371/JOURNAL.PONE.0223402

Kowalska-Krochmal, B., and Dudek-Wicher, R. (2021). The minimum inhibitory concentration of antibiotics: methods, interpretation, clinical relevance. *Pathogens* 10, 165–21. doi:10.3390/PATHOGENS10020165

Kremers, H. M., Larson, D. R., Crowson, C. S., Kremers, W. K., Washington, R. E., Steiner, C. A., et al. (2015). Prevalence of total hip and knee replacement in the United States. *J. Bone Jt. Surg. Am.* 97, 1386–1397. doi:10.2106/JBJS.N.01141

Li, C., Renz, N., and Trampuz, A. (2018). Management of periprosthetic joint infection. *Hip Pelvis* 30, 138–146. doi:10.5371/HP.2018.30.3.138

Li, K., Cuadra, M., Scarola, G., Odum, S., Otero, J., Griffin, W., et al. (2021). Complications in the treatment of periprosthetic joint infection of the hip: when do they occur? *J. Bone Jt. Infect.* 6, 295–303. doi:10.5194/JBJI-6-295-2021

Li, Z., Xu, C., and Chen, J. (2023). Articulating spacers: what are available and how to utilize them? *Arthroplasty* 5, 22. doi:10.1186/S42836-023-00167-6

Lunz, A., Knappe, K., Omlor, G. W., Schonhoff, M., Renkawitz, T., and Jaeger, S. (2022). Mechanical strength of antibiotic-loaded PMMA spacers in two-stage revision surgery. *BMC Musculoskelet. Disord.* 23, 945–949. doi:10.1186/s12891-022-05895-5

Macaulay, W., DiGiovanni, C. W., Restrepo, A., Saleh, K. J., Walsh, H., Crossett, L. S., et al. (2002). Differences in bone-cement porosity by vacuum mixing, centrifugation, and hand mixing. *J. Arthroplasty* 17, 569–575. doi:10.1054/arth.2002.32693

McConoughey, S. J., Howlin, R., Granger, J. F., Manring, M. M., Calhoun, J. H., Shirtliff, M., et al. (2014). Biofilms in periprosthetic orthopedic infections. *Future Microbiol.* 9, 987–1007. doi:10.2217/fmb.14.64

Messick, K. J., Miller, M. A., Damron, L. A., Race, A., Clarke, M. T., and Mann, K. A. (2007). Vacuum-mixing cement does not decrease overall porosity in cemented femoral stems: AN *in vitro* LABORATORY INVESTIGATION. *J. Bone Jt. Surg. Br.* 89, 1115–1121. doi:10.1302/0301-620x.89b8.19129

Minogue, T. D., Daligault, H. A., Davenport, K. W., Bishop-Lilly, K. A., Broomall, S. M., Bruce, D. C., et al. (2014). Complete genome assembly of *Escherichia coli* ATCC 25922, a serotype O6 reference strain. *Genome announc.* 2, e00969-14–983. doi:10.1128/GENOMEA.00969-14

Moore, K., Os, R. W. V., Dusane, D. H., Brooks, J. R., Delury, C., Aiken, S. S., et al. (2021). Elution kinetics from antibiotic-loaded calcium sulfate beads, antibiotic-loaded polymethacrylate spacers, and a powdered antibiotic bolus for surgical site infections in a novel *in vitro* draining knee model. *Antibiotics* 10, 270–10. doi:10.3390/ANTIBIOTICS10030270

Morgan, E. F., and Keaveny, T. M. (2001). Dependence of yield strain of human trabecular bone on anatomic site. *J. Biomech.* 34, 569–577. doi:10.1016/S0021-9290(01)00011-2

Nace, J., Siddiqi, A., Talmo, C. T., and Chen, A. F. (2019). Diagnosis and management of fungal periprosthetic joint infections. *J. Am. Acad. Orthop. Surg.* 27, e804–e818. doi:10.5435/JAAOS-D-18-00331

Pagac, M., Hajnys, J., Ma, Q. P., Jancar, L., Jansa, J., Stefek, P., et al. (2021). A review of vat photopolymerization technology: materials, applications, challenges, and future trends of 3D printing. *Polym. (Basel)* 13, 598–20. doi:10.3390/POLYM13040598

Painter, P. C., and Coleman, M. M. (2019). Fundamentals of polymer science: an introductory text. *Fundam. Polym. Sci.* doi:10.1201/9780203755211

Patra, S., Ajayan, P. M., and Narayanan, T. N. (2020). Dynamic mechanical analysis in materials science: the Novice's Tale. *Oxf. Open Mater. Sci.* 1. doi:10.1093/OXFMAT/ITAA001

Pelletier, M. H., Malisano, L., Smitham, P. J., Okamoto, K., and Walsh, W. R. (2009). The compressive properties of bone cements containing large doses of antibiotics. *J. Arthroplasty* 24, 454–460. doi:10.1016/j.arth.2007.10.023

Prince, N., Penatzer, J. A., Dietz, M. J., and Boyd, J. W. (2020). Localized cytokine responses to total knee arthroplasty and total knee revision complications. *J. Transl. Med.* 18, 330. doi:10.1186/S12967-020-02510-W

Rüdiger, H. A., Guillemin, M., Latypova, A., and Terrier, A. (2017). Effect of changes of femoral offset on abductor and joint reaction forces in total hip arthroplasty. *Arch. Orthop. Trauma Surg.* 137, 1579–1585. doi:10.1007/s00402-017-2788-6

Schut, J., Bolikal, D., Khan, I. J., Pesnell, A., Rege, A., Rojas, R., et al. (2007). Glass transition temperature prediction of polymers through the mass-per-flexible-bond principle. *Polym. Guildf.* 48, 6115–6124. doi:10.1016/J.POLYMER.2007.07.048

Seo, R. S., Vergani, C. E., Giampaolo, E. T., Pavarina, A. C., and Machado, A. L. (2007). Effect of a post-polymerization treatments on the flexural strength and Vickers hardness of reline and acrylic denture base resins. *J. Appl. Oral Sci.* 15, 506–511. doi:10.1590/S1678-77572007000600010

Shrestha, J., Zahra, F., and Cannady, P. (2023). Antimicrobial stewardship. *StatPearls*. Available online at: https://www.ncbi.nlm.nih.gov/books/NBK572068/(Accessed April 17, 2024).

Soni, I., Chakrapani, H., and Chopra, S. (2015). Draft genome sequence of methicillin-sensitive *Staphylococcus aureus* ATCC 29213. *Genome announc.* 3, e01095. doi:10.1128/GENOMEA.01095-15

Stavrakis, A. I., Niska, J. A., Loftin, A. H., Billi, F., and Bernthal, N. M. (2013). Understanding infection: a primer on animal models of periprosthetic joint infection. *Sci. World J.* 2013, 925906. doi:10.1155/2013/925906

Struelens, B., Claes, S., and Bellemans, J. (2013). Spacer-related problems in two-stage revision knee arthroplasty. *Acta Orthop. Belg* 79, 422–426.

Vancomycin hydrochloride (2023). Vancomycin hydrochloride (from Streptomyces orientalis), powder | VWR. Available online at: https://us.vwr.com/store/product/14514245/vancomycin-hydrochloride-from-streptomyces-orientalis-powder (Accessed March 6, 2023).

von Hertzberg-Boelch, S. P., Luedemann, M., Rudert, M., and Steinert, A. F. (2022). PMMA bone cement: antibiotic elution and mechanical properties in the context of clinical use. *Biomedicines* 10, 1830. doi:10.3390/BIOMEDICINES10081830

Vugt, T. A. G. van, Arts, J. J., and Geurts, J. A. P. (2019). Antibiotic-loaded polymethylmethacrylate beads and spacers in treatment of orthopedic infections and the role of biofilm formation. *Front. Microbiol.* 10, 1626. doi:10.3389/FMICB.2019.01626

Webb, J. C., Gbejuade, H., Lovering, A., and Spencer, R. (2013). Characterisation of *in vivo* release of gentamicin from polymethyl methacrylate cement using a novel method. *Int. Orthop.* 37, 2031–2036. doi:10.1007/S00264-013-1914-5

Xi, W., Hegde, V., Zoller, S. D., Park, H. Y., Hart, C. M., Kondo, T., et al. (2021). Point-of-care antimicrobial coating protects orthopaedic implants from bacterial challenge. *Nat. Commun.* 12, 5473. doi:10.1038/S41467-021-25383-Z

Yan, Y., Mao, Y., Li, B., and Zhou, P. (2020). Machinability of the thermoplastic polymers: PEEK, PI, and PMMA. *Polym. 2021* 13, 69–13. doi:10.3390/POLYM13010069

Zmistowski, B., Restrepo, C., Huang, R., Hozack, W. J., and Parvizi, J. (2012). Periprosthetic joint infection diagnosis: a complete understanding of white blood cell count and differential. *J. Arthroplasty* 27, 1589–1593. doi:10.1016/J.ARTH.2012.03.059